

# Accurate Computation of Electric Field Enhancement Factors for Metallic Nanoparticles Using the Discrete Dipole Approximation

A. Eugene DePrince · Robert J. Hinde

Received: 27 November 2009 / Accepted: 9 December 2009 / Published online: 29 January 2010  
© The Author(s) 2010. This article is published with open access at Springerlink.com

**Abstract** We model the response of nanoscale Ag prolate spheroids to an external uniform static electric field using simulations based on the discrete dipole approximation, in which the spheroid is represented as a collection of polarizable subunits. We compare the results of simulations that employ subunit polarizabilities derived from the Clausius–Mossotti relation with those of simulations that employ polarizabilities that include a local environmental correction for subunits near the spheroid’s surface [Rahmani et al. *Opt Lett* 27: 2118 (2002)]. The simulations that employ corrected polarizabilities give predictions in very good agreement with exact results obtained by solving Laplace’s equation. In contrast, simulations that employ uncorrected Clausius–Mossotti polarizabilities substantially underestimate the extent of the electric field “hot spot” near the spheroid’s sharp tip, and give predictions for the field enhancement factor near the tip that are 30 to 50% too small.

**Keywords** Metallic nanoparticles · Optical properties · Simulation

The electrical and optical properties of noble metal nanoparticles have attracted considerable scientific interest for many decades. Over a century ago, for example, Mie [1]—building on even earlier work by Lorenz [2] and possibly

others—attributed the colors of colloidal suspensions of Au nanoparticles [3] to the nanoparticles’ visible-wavelength optical scattering properties. Interest in the optical properties of noble metal nanoparticles has risen dramatically in recent years with the recognition that these properties, if understood in sufficient detail, can be harnessed to create nanoscale photonic devices and sensors.

The discrete dipole approximation [4, 5] (also called the coupled dipole approximation) is one of several numerical methods that have been developed to simulate the response of a small particle to an incident electromagnetic (EM) field. In simulations based on the discrete dipole approximation (DDA), a nanoparticle is modeled as a regular (typically cubic) lattice of polarizable subunits. The incident EM field induces dipole moments in each subunit; these dipole moments in turn generate local fields that further polarize nearby subunits. Once the subunits’ induced dipole moments are mutually self-consistent, the electromagnetic and optical properties of the dipole lattice are taken to mimic those of the real nanoparticle. The assumption that only dipolar interactions among subunits and between the subunits and the external field need be considered, an assumption that is implicit in DDA-based simulations, is generally thought to be a reasonable one provided that the subunits are small enough so that the electric field is nearly constant across an individual subunit; this assumption is frequently tested by comparing the results obtained from simulations at two or more levels of discretization.

The connection between the lattice of dipoles and the real nanoparticle is made through the choice of the polarizability tensor  $\alpha$  of the polarizable subunits. In the original formulation [4] of the DDA approach,  $\alpha$  was assumed to be an isotropic, diagonal tensor defined by the Clausius–Mossotti (CM) relation

A. E. DePrince · R. J. Hinde (✉)  
Department of Chemistry, The University of Tennessee,  
Knoxville, TN 37996-1600, USA  
e-mail: rhinde@utk.edu

*Present Address:*  
A. E. DePrince  
Department of Chemistry, The University of Chicago, Chicago,  
IL 60637, USA

$$\alpha = \frac{3}{4\pi\rho} \frac{\varepsilon - 1}{\varepsilon + 2} \tag{1}$$

where  $\rho$  is the number density of the polarizable subunits and  $\varepsilon$  is the nanoparticle’s dielectric constant; this relation is exact for an infinite cubic lattice of subunits in a zero-frequency external electric field [6]. For finite (nonzero) frequency external EM fields, a radiative reaction [6] correction to the zero-frequency polarizability tensor defined by Eq. 1 ensures that the optical theorem holds for the dipole lattice [5]. Other finite frequency corrections to the static polarizability given by Eq. 1 can be derived from an analysis of the dispersion relation for electromagnetic waves propagating along a lattice of polarizable points [7].

Real nanoparticles, of course, have surfaces, and hence cannot be represented as infinite lattices; consequently, the use of polarizabilities defined by Eq. 1 in DDA-based simulations of nanoparticles represents an additional approximation [8], one which persists even when the subunits are very small, which is not remediated by radiative reaction corrections or other finite frequency corrections, and which seems to be especially severe for materials whose dielectric constant has a large imaginary component [9]. Recent work [9, 10] suggests that the use of subunit polarizabilities that properly account for the anisotropic local environment of DDA subunits near surfaces can increase substantially the accuracy with which highly averaged far-field quantities, such as absorption and scattering cross-sections, can be computed using DDA-based methods. In this letter, we employ these corrected polarizabilities in DDA-based simulations of nanoscale Ag prolate spheroids in homogeneous static electric fields; we find that the new polarizabilities, which include a local environmental correction (LEC) to the CM polarizabilities, also substantially improve the description of spatially resolved near-field quantities, such as localized electric field enhancement factors, computed in these simulations.

We begin by summarizing some exact results obtained by solving Laplace’s equation for a homogeneous prolate spheroid in a uniform static external field [11, 12]; these are the benchmarks against which we assess the DDA-based simulations. We consider a prolate spheroid with major semiaxis  $c$  (henceforth assumed to coincide with the space-fixed  $z$  axis) and minor semiaxis  $a$ . The surface of the spheroid is one member of a family of confocal surfaces defined by the parameter  $\xi$ . These surfaces satisfy the equation

$$\frac{x^2 + y^2}{a^2 + \xi} + \frac{z^2}{c^2 + \xi} = 1; \tag{2}$$

the surface of the spheroid corresponds to  $\xi = 0$ . If such a spheroid, with dielectric constant  $\varepsilon$ , is immersed in a medium with dielectric constant  $\varepsilon_m$  and exposed to a uniform static

electric field  $\mathbf{E}_{\text{ext}} = E_0\hat{\mathbf{z}}$  parallel to the space-fixed  $z$  axis, the electrical potential at any point outside the spheroid is given by

$$\Phi_{\text{out}} = -E_0z \left[ 1 - \frac{sL_z(\xi)}{1 + sL_z(0)} \right] \tag{3}$$

where  $s = (\varepsilon - \varepsilon_m)/\varepsilon_m$  and  $L_z(\xi)$  is the dimensionless integral

$$L_z(\xi) = \frac{a^2c}{2} \int_{\xi}^{\infty} \frac{du}{(u + a^2)(u + c^2)^{3/2}}. \tag{4}$$

The integral  $L_z(0)$  can be computed analytically:

$$L_z(0) = \frac{1 - e^2}{e^2} \left( -1 + \frac{1}{2e} \ln \frac{1 + e}{1 - e} \right) \tag{5}$$

where the spheroid’s eccentricity  $e = \sqrt{1 - (a/c)^2}$ . The potential inside the spheroid is given by

$$\Phi_{\text{in}} = -\frac{E_0z}{1 + sL_z(0)}. \tag{6}$$

It is clear from this equation that the field inside the spheroid is uniform and parallel to the external field. In addition, the polarization  $\mathbf{P}$  (dipole moment per unit volume) inside the spheroid is uniform and is given by

$$\mathbf{P} = \frac{\varepsilon_0(\varepsilon - 1)}{1 + sL_z(0)} E_0\hat{\mathbf{z}} \tag{7}$$

where  $\varepsilon_0$  is the absolute permittivity of free space.

The electric field outside the spheroid is  $\mathbf{E} = -\nabla\Phi_{\text{out}}$ ; for points on the  $z$  axis,

$$\mathbf{E} = \left[ 1 + \frac{s}{1 + sL_z(0)} \left( \frac{a^2c}{z(z^2 + a^2 - c^2)} - L_z(\xi) \right) \right] E_0\hat{\mathbf{z}}. \tag{8}$$

The quantity in square brackets in this equation is the on-axis electric field enhancement factor, which we henceforth denote as  $F$ . It has the value  $F_{\text{tip}} = (1 + s)/[1 + sL_z(0)]$  at the spheroid’s tip  $(x, y, z) = (0, 0, c)$ , and approaches  $F = 1$  as  $z \rightarrow \infty$ . Large  $F_{\text{tip}}$  values can be achieved when the quantity  $1 + sL_z(0)$ , which is controlled by the spheroid’s aspect ratio  $c/a$  and dielectric constant, is small in magnitude.

We now turn to our DDA-based simulations. The technical aspects of these simulations have been extensively reviewed [5, 13]; we therefore report only those computational details that are specific to the simulations presented here. We model a spheroid as a collection of  $N$  contiguous cubic subunits, with edges of length  $d$ , centered at the positions  $(x, y, z) = (n_x d, n_y d, n_z d)$ ; here,  $(n_x, n_y, n_z)$  is an integer triple that satisfies  $c^2(n_x^2 + n_y^2)/a^2 + n_z^2 \leq n_{\text{max}}^2$ , where  $n_{\text{max}}$  is an integer that determines the discretization level of the spheroid. The edge length  $d$  is chosen so that the

volume enclosed by the collection of cubic subunits is equal to the spheroid volume. The linear algebraic equations that determine the dipole moments  $\mathbf{m}_j$  of the individual subunits (here  $j$  is an index that distinguishes individual subunits) are solved using the complex-arithmetic implementation of the GMRES algorithm described by Frayssé et al. [14]; we terminate the algorithm and record the dipole moments  $\mathbf{m}_j$  once the normwise backward error drops below  $10^{-6}$ . We obtain the wavelength-dependent dielectric function of Ag via linear interpolation of the data points compiled by Lynch and Hunter [15]; as our main goal in the present work is not to provide results for comparison with experiment, but to compare the accuracy of the results obtained in simulations with and without the local environmental correction to the polarizabilities, we neglect finite-size corrections to the dielectric constant that arise from electronic scattering from the spheroid surface [16]. Henceforth, we set  $\epsilon_m = 1$  (corresponding to vacuum as the medium surrounding the spheroid) and  $E_0 = 1$  au; all of the results we report are scaled by  $1/E_0$ , so the numerical value of  $E_0$  is ultimately irrelevant.

First, we examine the polarization  $\mathbf{P}$  induced in a metallic nanoparticle by a uniform static external electric field. We consider a prolate spheroid with  $a = 10$  nm,  $c = 40$  nm, and dielectric constant  $\epsilon = 12.26 + 0.84i$  (corresponding to an excitation wavelength of  $\lambda \approx 570$  nm). For this aspect ratio and dielectric constant, the quantity  $1 + sL_z(0)$  is purely imaginary and small in magnitude:  $1 + sL_z(0) \approx 0.0633i$ . We use the DDA to simulate this spheroid at several levels of discretization, ranging from  $N = 6041$  subunits ( $d = 1.405$  nm) to  $N = 24679$  subunits ( $d = 0.879$  nm). We divide the dipole moment  $\mathbf{m}_j$  of each subunit by the subunit volume  $d^3$  to obtain the polarization  $\mathbf{P}_j$  for each subunit; we then divide the magnitude of this vector by the magnitude of the exact polarization vector defined in Eq. 7 to obtain a dimensionless relative polarization  $\tilde{P}_j$  for each subunit. This quantity has the value  $\tilde{P}_j = 1$  when the magnitude of a subunit's dipole moment  $\mathbf{m}_j$  is consistent with the exact uniform polarization given by Eq. 7.

For DDA-based simulations employing CM polarizabilities, Fig. 1 shows how the mean and standard deviation of  $\tilde{P}_j$ , evaluated over the  $N$  subunits in a given spheroid, depend on the subunit edge length  $d$ . We see that for all of the spheroids considered here, the mean  $\tilde{P}_j$  value differs considerably from the value  $\tilde{P}_j = 1$ . For each spheroid, the standard deviation of the  $\tilde{P}_j$  values is about 0.2, indicating that the polarization within the spheroid is rather nonuniform—in contrast to the exact result given by Eq. 7—and does not become more uniform as the subunits become smaller; for two of the spheroids, Fig. 2 depicts graphically the large subunit-to-subunit variations in  $\tilde{P}_j$  that are observed using CM polarizabilities. By comparison,

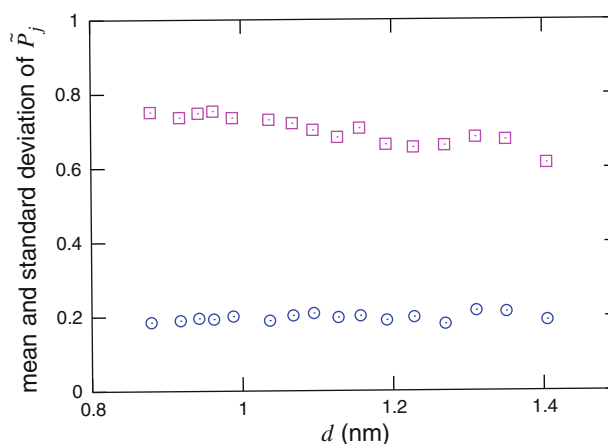


**Fig. 1** Mean (boxes) and SD (circles) of the relative subunit polarizations  $\tilde{P}_j$ , as a function of subunit edge length  $d$ , for DDA-based simulations of a prolate Ag spheroid with semiaxes  $a = 10$  nm and  $c = 40$  nm; the simulations employ uncorrected CM polarizabilities

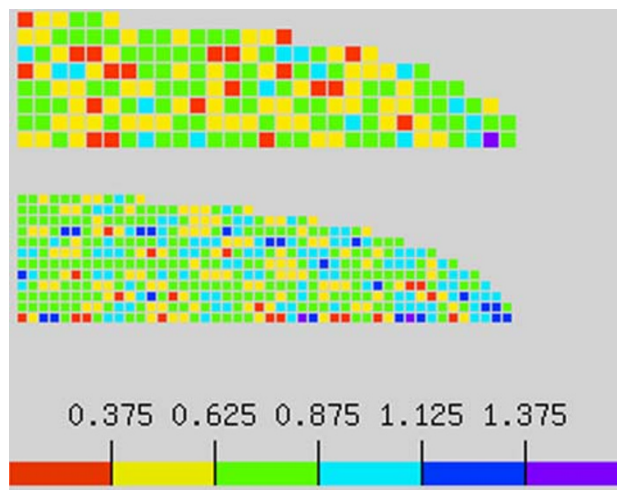


**Fig. 2** Relative polarizations  $\tilde{P}_j$  derived from DDA-based simulations of a prolate Ag spheroid with semiaxes  $a = 10$  nm and  $c = 40$  nm; the simulations employ uncorrected CM polarizabilities. Each subunit is represented by a square colored according to the relative polarization scale shown at the bottom of the figure. The upper panel gives the results for a spheroid modeled using  $N = 6041$  subunits of edge length  $d = 1.405$  nm; the lower panel gives the results for  $N = 24679$  subunits of edge length  $d = 0.879$  nm. Only subunits with  $x = 0$ ,  $y \geq 0$ , and  $z \geq 0$  are shown

when we use the subunit polarizabilities of [8] that include the LEC, our DDA-based simulations produce subunit dipole moments that give  $\tilde{P}_j = 1$  for each subunit in the spheroid, indicating that the magnitudes of the dipole moments are in exact agreement with Eq. 7. This is not much of a surprise, because the corrected polarizabilities given by Rahmani et al. [8] are defined so that, when used in DDA-based simulations, they reproduce exactly the

position-dependent polarization inside an object immersed in a static external electric field [8, 9]. What Figs. 1 and 2 show is that DDA-based simulations that use CM polarizabilities may fail in this regard, and that this failure is not simply a result of the discretization that necessarily accompanies the DDA.

We now examine the near-field properties of the Ag nanoparticle, focusing on the localized enhancement of the applied electric field near the nanoparticle's surface. Figure 3a compares the magnitude  $|F|$  of the exact on-axis electric field enhancement factor  $F$  [which is a complex quantity because  $\varepsilon$  is complex; see Eq. 8] near the spheroid's sharp tip with the DDA-based results obtained for  $N = 24679$  subunits using both CM and LEC polarizabilities. The enhancement factor computed using LEC polarizabilities is in good agreement with the exact result, even at points within 0.4 nm (which is less than one-half of the subunit separation  $d$ ) of the spheroid's surface (the electric field varies discontinuously across the spheroid's surface, and no DDA-based simulation will be able to model this discontinuous change; it is therefore unreasonable to expect these simulations to give accurate  $|F|$  values just outside the spheroid's surface). By contrast, the simulation that employs CM polarizabilities substantially underestimates  $|F|$ . In Fig. 3b, we show how the values of  $|F|$  computed at  $z = 41$  nm (1 nm away from the sharp tip) vary with  $d$  over the range of discretizations considered here; although the  $|F|$  values computed using CM polarizabilities vary slightly as  $d$  decreases, it appears that very small subunits will be needed before the CM result approaches the exact one. On the other hand, the  $|F|$  values computed using LEC polarizabilities are within a few percent of the exact result at all levels of discretization.

To gain more insight into the relative performance of DDA-based simulations employing CM and LEC polarizabilities, we use the simulations to compute the electric field enhancement factor in the vicinity of the spheroid's sharp tip, and compare these enhancement factors to reference results obtained by numerically differentiating the exact electrical potential  $\Phi_{\text{out}}$  defined in Eq. 3. To partially mitigate the discretization effects that are inherent in DDA-based simulations, we rotationally average the field enhancement factor obtained from these simulations by computing it on ten evenly spaced dihedral planes containing the space-fixed  $z$  axis and then averaging the enhancement factors obtained for each dihedral plane.

Fig. 4 shows, for  $N = 24679$  subunits, how the magnitudes of the enhancement factors computed using DDA-based simulations compare with the reference results derived from Eq. 3. Although neither of the DDA-based simulations can predict accurately the field enhancement factors at the surface of the spheroid (because the electric field varies discontinuously across the spheroid's surface,

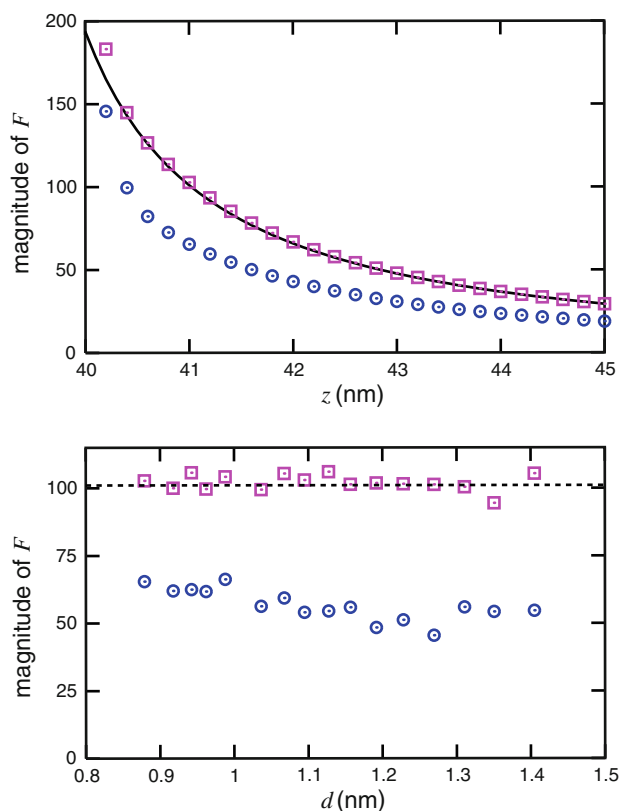


**Fig. 3** Magnitude of  $F$ , the on-axis electric field enhancement factor, for a prolate Ag spheroid with semiaxes  $a = 10$  nm and  $c = 40$  nm. **a** Dependence of  $|F|$  on position  $z$ ; the point  $z = 40$  nm is at the spheroid's sharp tip. *Solid line* gives the exact result of Eq. 8; *boxes* and *circles* give the results of DDA-based simulations with  $N = 24679$  subunits employing LEC and CM polarizabilities, respectively. **b** Dependence of  $|F|$  at  $z = 41$  nm on the edge length  $d$  of the DDA subunits. The *dotted line* at  $|F| = 102.7$  gives the exact result of Eq. 8; *boxes* and *circles* give the results of DDA-based simulations employing LEC and CM polarizabilities, respectively

as previously noted), the shape, size, and internal structure of the spheroid's near-field hot spot are modeled fairly well by the simulations that employ LEC polarizabilities. The DDA-based simulations that employ CM polarizabilities, by contrast, yield a hot spot that is too small and whose peak intensity is too low.

In summary, we have modeled the response of a nanoscale Ag prolate spheroid to an external electric field using DDA-based simulations that employ subunit polarizabilities that either include or omit a local environmental correction. We invoke the electrostatic approximation, in which the incident field is assumed to be spatially uniform and static, but the spheroid's dielectric constants is taken from the wavelength-dependent dielectric function of bulk Ag; this allows us to compare the predictions of the DDA-based simulations to exact results obtained by solving Laplace's equation for prolate spheroids in a uniform static external field. We have chosen a dielectric constant for the

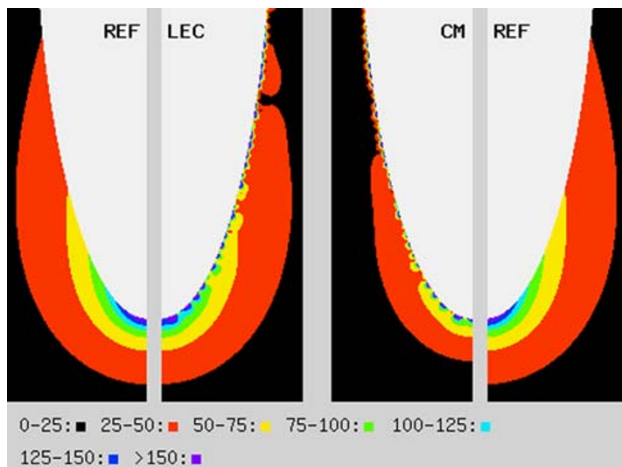


**Fig. 4** Magnitude of the electric field enhancement factor near the sharp tip of a prolate Ag spheroid with semiaxes  $a = 10$  nm and  $c = 40$  nm. Panels marked “REF” are reference results obtained by differentiating Eq. 3; “CM” and “LEC” indicate the results of DDA-based simulations employing CM and LEC polarizabilities, respectively. The DDA-based simulations use  $N = 24679$  subunits of edge length  $d = 0.879$  nm to model the spheroid; the colored squares in the legend at the bottom of the figure are scaled to have the same edge length

spheroid that maximizes the electric field enhancement factor at the spheroid’s sharp tip. The predictions of DDA-based simulations that employ LEC polarizabilities are much closer to the exact results than are those of DDA-based simulations that employ CM polarizabilities; simulations using CM polarizabilities yield a near-field hot spot that is too small and field enhancement factors that are too low. We therefore conclude that DDA-based simulations of metallic nanoparticles that employ uncorrected CM polarizabilities may give inaccurate predictions of the particle’s spatially resolved near-field properties, even at locations some distance away from the particle’s surface.

**Acknowledgments** This work was supported by grants from the University of Tennessee Honors Program (A.E.D.) and the US Department of Energy (R.J.H.). R.J.H. thanks L. Blocker, L. Dixon, and E. Read (University of Tennessee Libraries) for bibliographic assistance.

**Open Access** This article is distributed under the terms of the Creative Commons Attribution Noncommercial License which permits any noncommercial use, distribution, and reproduction in any medium, provided the original author(s) and source are credited.

## References

1. G. Mie, Ann. Phys. Leipz. **25**, 377 (1908)
2. L.V. Lorenz, Det Kongelige Danske videnskabernes selskabs **6**(6), 1 (1890)
3. M. Faraday, Phil. Trans. R. Soc. Lond. **147**, 145 (1857)
4. E.M. Purcell, C.R. Pennypacker, Astrophys. J. **186**, 705 (1973)
5. B.T. Draine, Astrophys. J. **333**, 848 (1988)
6. J.D. Jackson, *Classical electrodynamics* (Wiley, New York, 1999)
7. B.T. Draine, J. Goodman, Astrophys. J. **405**, 685 (1993)
8. A. Rahmani, P.C. Chaumet, G.W. Bryant, Opt. Lett. **27**, 2118 (2002)
9. A. Rahmani, P.C. Chaumet, G.W. Bryant, Astrophys. J. **607**, 873 (2004)
10. M.J. Collinge, B.T. Draine, J. Opt. Soc. Am. A **10**, 2023 (2004)
11. J.A. Stratton, *Electromagnetic theory* (Mc-Graw Hill, New York, 1941)
12. C.F. Bohren, D.R. Huffman, *Absorption and scattering of light by small particles* (Wiley, New York, 1983)
13. B.T. Draine, P.J. Flatau, J. Opt. Soc. Am. A **11**, 1491 (1994)
14. V. Frayssé, L. Girard, S. Gratton, J. Langou, ACM Trans. Math. Soft. **21**, 228 (2005)
15. D.W. Lynch, W.R. Hunter, in *Handbook of optical constants of solids*, ed. by E.D. Pali (Academic, San Diego, 1985). Part II, Subpart 1
16. W.A. Kraus, G.C. Schatz, J. Chem. Phys. **79**, 6120 (1983)